Effective Knudsen Diffusivities in Structures of Randomly Overlapping Fibers

Manolis M. Tomadakis and Stratis V. Sotirchos
Dept. of Chemical Engineering, University of Rochester, Rochester, NY 14627

Effective Knudsen diffusion coefficients are presented for fibrous structures consisting of overlapping fibers. The fibers are distributed randomly in d (d = 2 or 3) directions with their axes perpendicular to one direction (d = 2) or in the three-dimensional space with no preferred orientation (d = 3), or they are grouped into d (d = 1, 2, or 3) mutually perpendicular bundles of parallel, randomly overlapping fibers. Effective diffusivities are computed using a Monte Carlo simulation scheme to determine the mean square displacement of molecules traveling in the interior of the porous medium for large travel times. Our results show that structures with fibers distributed randomly in d directions have diffusion coefficients identical, within the accuracy of our simulation, to those of d-directional, parallel fiber structures. Effective Knudsen diffusivities are strongly influenced only by the directionality of the fiber structure, with tridirectional or randomly oriented fiber structures presenting lower percolation thresholds (0.04 vs. 0.11) and higher effective diffusivities than bidirectional or random structures with their axes perpendicular to one direction. The tortuosity factor is in general found to decrease with increasing porosity, approaching for each case, as the porosity goes to unity, the corresponding lower bound that is derived using variational principles.

Introduction

Porous media with a solid phase that consists of or can be represented by a structure of solid fibers are encountered in numerous practical applications, ranging from thermal insulation materials to filters for gases or liquids. Fibrous structures are also involved, as starting materials, in the manufacture of fiber-reinforced composites for structural applications. The use of fiber-reinforced composites in commercial applications has undergone a dramatic expansion over the last two decades, and many of these materials now find use in products that range from advanced aircraft to sporting goods. Fiber-reinforced ceramic-ceramic composites, in particular, are especially attractive for high-temperature applications such as exhaust cones and nozzles in rockets, heat shields, and brake disks for supersonic aircraft and race cars.

Diffusion of gases in fiber structures is the process that controls diffusion-driven chemical vapor infiltration (CVI), the most developed method for producing fiber-reinforced ceramic composites (Stinton et al., 1988). During this process, gaseous reactants or the products of their thermal decomposition are transported by diffusion to the interior of the fibrous preform, where they react to deposit a ceramic material on the surface of the fibers. If the rate of chemical reaction is relatively higher than that of mass transport, significant concentration gradients may be present in the densifying structure, leading in turn to nonuniform reaction rates and significant density (or equivalently, porosity) gradients. Eventually, this may culminate in complete sealing of the external surface of the preform, preventing further densification of the interior. Using a mathematical model describing diffusion and reaction during chemical vapor infiltration, it is possible to determine optimal reaction conditions for obtaining products of acceptable density gradients and reducing the processing time (Sotirchos and Tomadakis, 1990). However, knowledge of the variation of the effective diffusion coefficient and of the structural properties of the preform with the conversion is needed for such an analysis, in addition to the kinetics of the reaction.

Correspondence concerning this paper should be addressed to S. V. Sotirchos.

The variation of the effective Knudsen diffusion coefficient with the porosity in a class of fiber structures is the subject of our study. We consider fiber structures formed by cylindrical fibers distributed randomly in d (d = 2 or 3) directions (d-directional, random-fiber structures), that is, with their axes perpendicular to one direction (d = 2) or in the three-dimensional space without preferred orientation (d=3). We also consider fibrous structures in which the fibers are grouped into d (d = 1, 2, or 3) bundles of parallel, randomly overlapping fibers, with the bundles arranged in mutually perpendicular directions (d-directional, parallel-fiber structures). Unidirectional fiber structures may be viewed as representative of preforms consisting of parallel fibers. Bidirectional fiber structures or structures with fibers distributed randomly in two directions, on the other hand, have the fibers arranged with their axes perpendicular to one direction, and consequently, they may be used as physical models of preforms made of cloth layups. Although the fiber structures encountered in most practical applications are not randomly overlapping, structures of randomly overlapping fibers possess a number of special features that make them particularly attractive, especially for computer simulation. They permit a straightforward construction of finite samples of the porous medium, and they provide explicit expressions for the variation of their structural properties with the porosity and fiber size distribution, which can be used to check whether the finite sample is statistically representative of the infinite porous medium. Parallel, d-directional fiber structures have the additional advantage that they are compatible with periodic boundary conditions, making possible the construction of finite periodic samples that span the three-dimensional space.

The effective Knudsen diffusion coefficients in the fiber structures are computed by means of a Monte Carlo simulation method. It rests in computing the trajectories of a large number of molecules introduced randomly in a finite sample (unit cell) of the fiber structure and using them to compute the mean square displacement of the molecules from their initial positions for large travel times. The effective diffusivity is then found from the mean square displacement equation (Kennard, 1938; Rahman, 1964), appropriately modified to account for the presence of the solid phase. The information from the molecular trajectory computations is also used to determine the variation of the accessible structural properties of the solid (e.g., surface area and porosity) with the total porosity. The method can be used for any porous medium and in the transition and bulk diffusion regimes as well. Burganos and Sotirchos (1989a) used it to compute effective diffusivities in structures of randomly overlapping capillaries of various orientation distributions. In order to check the results of the mean square displacement method, effective diffusivities for a few cases will also be determined using the transmission probability method, in which the molecular trajectories are used to compute the transmission probability of molecules through a pair of parallel planes, normal to the direction of diffusion (Burganos and Sotirchos, 1988, 1989a). A brief description of the procedures used for constructing finite samples of fiber structures and computing molecular trajectories is given in the following section.

Past work on Knudsen diffusion in overlapping fiber structures has primarily been focused on the derivation of upper bounds using variational principles (Faley and Strieder, 1987, 1988). Some numerical results on the effective Knudsen diffusivity for the case of randomly oriented fibers, obtained using the transmission probability method, were recently presented by Melkote and Jensen (1989). The results of these studies will be discussed during the presentation of our results.

Fiber Structures Construction and Computation of Effective Knudsen Diffusivities

The construction of a finite sample for a porous structure consisting of mutually perpendicular families of parallel, randomly overlapping fibers is a process entirely analogous to that discussed in detail by Burganos and Sotirchos (1988, 1989a) for the corresponding capillary structures. The same observation also holds for the construction of samples for structures consisting of fibers oriented randomly in two or three directions. Burganos and Sotirchos based the construction of each bundle in their multidirectional pore structures on the number of pores that lie in or intersect the finite sample of the structure. For periodic samples, the construction procedure can be simplified by considering only the fibers (or pores) with axes lying in the finite sample. The positions of these fibers are readily determined by considering a random distribution of points, as many as the fibers, on one of the two faces of the cubic finite sample that are perpendicular to the direction of the fibers. By repeating the same distribution of points on the corresponding faces of the neighboring cells and treating the points as the traces of the axes of the fibers, a structure of parallel, randomly overlapping fibers spanning the whole space in directions perpendicular to the fibers is obtained. This procedure is repeated for all d bundles in a d-directional structure.

A periodic, unidirectional structure of uniformly sized fibers constructed by the above procedure is shown in Figure 1. The

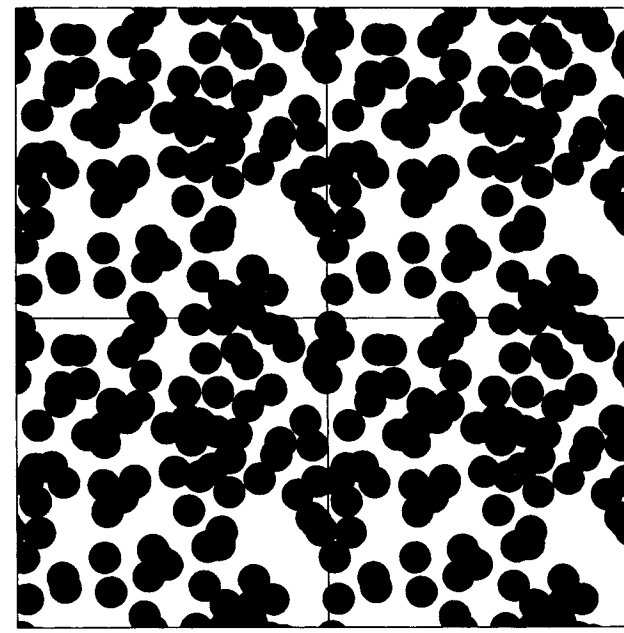

Figure 1. Section of four periodic neighboring cells of a unidirectional periodic fiber structure, perpendicular to fibers.

r/a = 0.05; ϵ = 0.5

figure presents sections of four adjacent cells with a plane perpendicular to the direction of the fibers for 50% porosity and a unit cell side to fiber radius ratio equal to 20. The section of a structure of randomly oriented fibers is shown in Figure 2 for the same porosity and unit cell side to fiber radius ratio as the structure of Figure 1. For fibers of 1 μm radius, Figures 1 and 2 depict 20 $\times$ 20 μm sections of the fiber structures.

Structures of randomly oriented fibers are constructed by distributing randomly in three directions the axes of the fibers that intersect the unit cell of the structure (Burganos and Sotirchos, 1989a). If the axes of the fibers are distributed randomly in two directions only—that is, are kept parallel to a pair of faces of the unit cell—an anisotropic fiber structure, the randomly oriented analog of the bidirectional, parallel-fiber structure is obtained. Construction of periodic unit cells for randomly oriented structures, in both three and two directions, is impossible. In order to avoid working with very large samples, it is assumed that in the case of randomly oriented fibers, the infinite porous medium consists of identical unit cells, cubic with side a, arranged in such a way that any two neighboring cells are mirror images of each other with respect to their common face. The resulting structure can also be viewed as a periodic, space-filling scheme employing cubic unit cells of side $2a$. The construction of randomly oriented fiber structures (in two or three directions) is more involved than that of parallel fiber structures, but in both cases the computational effort required for constructing the unit cell is negligible in comparison to the time needed for computing the effective diffusivity.

Burganos and Sotirchos (1989a) presented expressions for the dependence of the porosity, ϵ, and surface area, S, of the finite samples of multidirectional, parallel-pore structures on the radius and number density of the pores. Since the porosity of a fiber structure is equivalent to the solid fraction of a pore structure, these expressions may readily be transformed to the corresponding expressions for the structural properties of fiber structures by simply replacing $(1-\epsilon)$ by ϵ. For infinitely large samples, the porosity and surface area of an n-modal, discrete random fiber structure are given by the relations

$$\epsilon = \exp\left(-\pi \sum_{i=1}^{n} l_i r_i^2\right) \tag{1}$$

$$S = 2\pi\epsilon \sum_{i=1}^{n} l_i r_i \tag{2}$$

with l_i being the length of axes of fibers with radius r_i per unit volume. It is clear from the form of Eqs. 1 and 2 that the average structural properties of the random-fiber structures are independent of the distribution of their orientation. For a d-directional fiber structure consisting of d statistically identical bundles, l_i/d is the number of traces of fiber axes per unit area on the faces of the unit cell that are perpendicular to one of the bundles.

Effective Knudsen diffusivities in the above structure are computed by means of a Monte Carlo simulation procedure using the mean square displacement, $<\xi^2>$, of a large number of molecules, introduced randomly in the unit cell, for large values of travel time, τ. $<\xi^2>$ is used to obtain the orientationally averaged effective diffusivity, D_e, while the mean square component of the displacement in the x, y, or z direction, $<\xi^2_{x,y, \text{ or } z}>$, gives the effective Knudsen diffusivities associated with diffusion in these directions. The expressions used are (Kennard, 1938; Rahman, 1964):

$$D_e = \frac{<\xi^2>}{6\tau} \tag{3a}$$

$$D_{e(x,y, \text{ or } z)} = \frac{<\xi^2_{x,y, \text{ or } z}>}{2\tau} \tag{3b}$$

In order to test the results of the mean square displacement method, effective diffusivities in a given direction were computed for a few cases using Monte Carlo estimates of the transmission probability of molecules traveling in the fiber structure, that is, the probability that molecules passing a plane perpendicular to the direction of diffusion will be transmitted through another plane that is parallel to the first and located at some known distance from it (Abbasi, 1981; Burganos and Sotirchos, 1988).

The trajectories of the molecules in the fiber structures are followed using a computational procedure similar to that presented in detail by Burganos and Sotirchos in previous publications (1988, 1989a). The molecules are assumed to undergo diffuse reflections at the walls of the fibers. In order to locate the next collision of a molecule, we find all potential intersections of the straight path followed by the molecule with the fiber walls and the boundaries of the unit cell. The position of the next collision of the molecule is then taken as the closest intersection to the position of the last collision. If the closest intersection happens to be with one of the faces of the unit cell, the molecule is allowed to move, retaining its direction

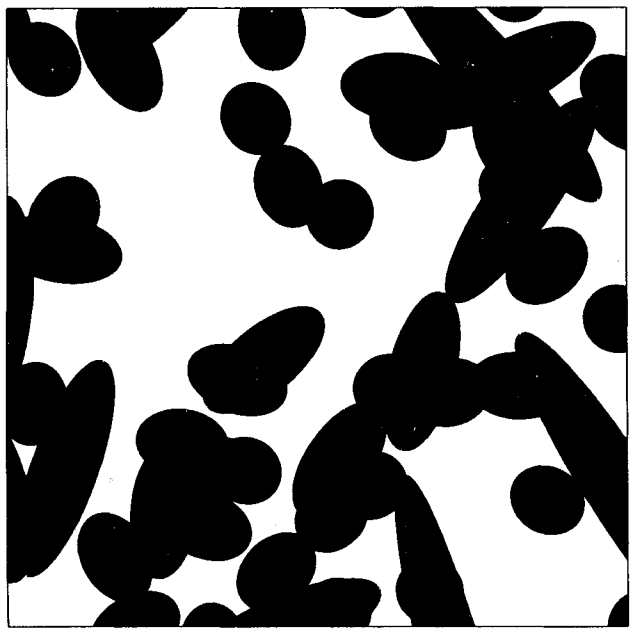

Figure 2. Section of unit cell of a structure of fibers randomly oriented in three directions.

$r/a = 0.05$; $\epsilon = 0.5$

of travel, into the adjacent cell, which is either identical to the original one (d-directional, parallel-fiber structures) or its mirror image relative to the face at which 'collision took' place (d-directional, random-fiber structures).

Results and Discussion

Effective diffusivity results

The results presented and discussed in this section are for fiber structures consisting of fibers of uniform size (unimodal). The computer simulation results for the effective Knudsen diffusivities in directions parallel (D_{ez}) and perpendicular ($D_{ex\text{ or }y}$) to the fibers of a unidirectional, unimodal fiber structure are shown in Figure 3. Shown there is also the orientationally averaged effective diffusivity (D_e) of this anisotropic fiber structure, Eq. 3a. The diffusivities reported in Figure 3 and all other figures have been rendered dimensionless and independent of the fiber size using as reference value the Knudsen diffusivity in a pore of radius equal to the fiber radius, $D(r) = (2/3)r\bar{v}$.

The data points shown in the figures represent simulation results for different random realizations of the fiber structures, with each point obtained from a single realization. The porosity of the fiber structures was varied by changing the population density of the fibers (l_i in Eq. 1), keeping the fiber radius to the unit cell side ratio, r/a, constant, or conversely by keeping the population density constant and changing the ratio r/a. Fiber radius to unit cell side ratios ranging from 0.01 to 0.07 were employed in our computations, and the number of fibers used ranged from 200 to 1,200 per cell. The total number of molecules that was introduced in the unit cell was varied with the porosity of the realization so that the number of molecules that fell in the void space of the structure was about 500. The sensitivity of the simulation results to the realization increased with increasing r/a, but the porosity of the structures proved to be the only factor that systematically influenced the predicted effective diffusivities. Since each data point shown in Figures 3, 6, 7, and 9 was obtained from a single realization, information on the statistical error involved in our simulations may be obtained from direct inspection of the figures. Away from the percolation threshold, the average statistical error—as the results of the figures show—varied from about 20% at low porosities to less than 5% in the high-porosity region. Since the effective diffusivity decreased precipitously in the vicinity of the percolation threshold, the relative statistical error was much higher in this region. One of the worst cases may be seen in Figure 7 for diffusion perpendicular to the fibers of a bidirectional fiber structure, where the estimated effective diffusivity at 0.14 porosity for the seven realizations shown in the figure ranged from 1.1×10^{-3} to 3.4×10^{-3}.

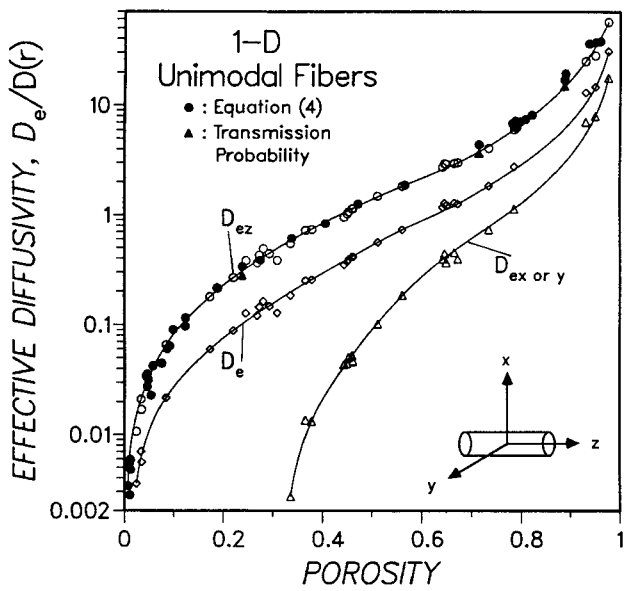

Figure 3. Effective Knudsen diffusivities for a unidirectional fiber structure.

D_{ez}, parallel to fiber axes, D_{ex} and D_{ey}, perpendicular to fiber axes
D_e orientationally averaged value

The results for the effective diffusivities in the z direction that are represented using filled circles were computed by means of an expression for diffusion in tubes of nonreentrant shape, that is, with walls parallel to the direction of diffusion, given by Kennard (1938). According to this expression, the effective diffusivity in the z direction is given by

$$D_{ez} = \frac{\bar{v}}{8A} \int_A \int_0^{2\pi} s d\phi dA \tag{4}$$

where A is the cross-sectional area of the unit cell and s is the distance from the area element dA to the walls of the fiber structure on the plane of the cross section at an angle ϕ with respect to some reference line. For points lying in the solid phase, s is obviously equal to zero. A Monte Carlo simulation scheme (Burganos and Sotirchos, 1988) was used to compute the double integral of Eq. 4. As the results of Figure 3 show, the diffusion coefficients of Eq. 4 are in excellent agreement with those of the mean square displacement method. This was also found to be the case for the effective diffusivities obtained using the transmission probability method. Results obtained using this method are shown by solid triangles in Figure 3.

The shape of the $D_{ex\text{ or }y}$ vs. ϵ curve reveals the existence of a percolation threshold for diffusion in directions perpendicular to the fibers. Our computations located this threshold at about 33% porosity, in agreement with the 66–67% percolation threshold reported by Burganos and Sotirchos (1988) for diffusion in unidirectional capillary structures. For porosities below this threshold value, there exists no infinitely large subset of the void space that spans the fibrous structure in directions perpendicular to the fibers, and as a result, the corresponding effective diffusivities D_{ex} and D_{ey} are identically equal to zero.

The effective diffusivities of Figure 3 for diffusion in directions parallel (D_{ez}) and perpendicular ($D_{ex\text{ or }y}$) to the fibers of a unidirectional fiber structure are compared in Figure 4 with the corresponding effective diffusion coefficients of a unimodal, unidirectional pore structure that were reported by Burganos and Sotirchos (1988). One should note the different location of the percolation threshold for diffusion perpendicular to the directions of the fibers or pores. We also observe that pore structures exhibit lower diffusivities than fiber structures of the same porosity (for fibers and pores of the same radius), with the exception of D_{ez} in the region of low porosities. A partial explanation for this behavior may be obtained by considering the variation of the mean intercept lengths of

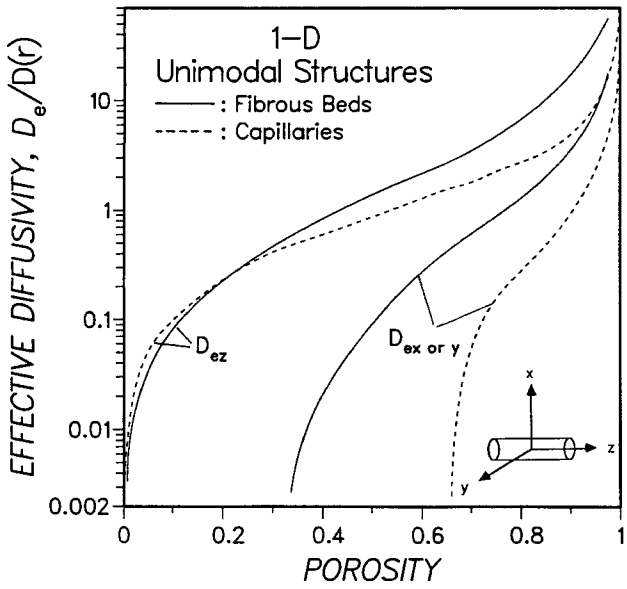

Figure 4. Effective diffusivities of unidirectional fiber structures and unidirectional pore structures.

the pore and fiber structures ($4\epsilon/S$), that is, the mean distance traveled between molecule-wall collisions, with the porosity. It can be shown using Eqs. 1 and 2 that the mean intercept length of structures of fibers of uniform size, $\bar{d}$, is given by the expression

$$\frac{\bar{d}}{r} = \frac{4\epsilon}{Sr} = \frac{-2}{\ln\epsilon} \tag{5}$$

The corresponding expressions for the pore structures, on the other hand, give

$$\frac{\bar{d}}{r} = \frac{4\epsilon}{Sr} = \frac{-2\epsilon}{(1-\epsilon)\ln(1-\epsilon)} \tag{6}$$

The above equations state that as the porosity goes to zero, the dimensionless mean intercept length approaches zero for fibers but converges to 2 for pores (the diameter of the pores). In view of this result, it is not surprising that pore structures present lower diffusional resistance at low porosities. The mean intercept length for fiber structures remains smaller than that for pore structures up to 0.5 porosity, while at higher porosities the opposite relationship holds.

The Knudsen diffusivity based on the average pore radius $\bar{r} = \bar{d}/2$ can be used to construct a correlation for the effective Knudsen diffusivity of a porous medium of the form

$$D_e = \frac{\epsilon}{\eta} D(\bar{r}) \tag{7a}$$

$$\frac{D_e}{D(r)} = \frac{\epsilon}{2\eta}\frac{\bar{d}}{r} \tag{7b}$$

where η is the tortuosity factor. The dimensionless effective diffusivities predicted by Eq. 7b for $\eta = 3$ (a commonly used approximation of the effective Knudsen diffusivity of porous media) are compared in Figure 5 with the orientationally averaged effective diffusivities for structures of unidirectional fibers, Figure 3, and unidirectional pores (Burganos and Sotirchos, 1988). It is seen that the tortuosity factor of unidirectional fiber or pore structures, based on $D(\bar{r})$, is smaller than 3 at all porosities. For pore structures, it asymptotically approaches 3 as the porosity goes to zero. Pore overlapping

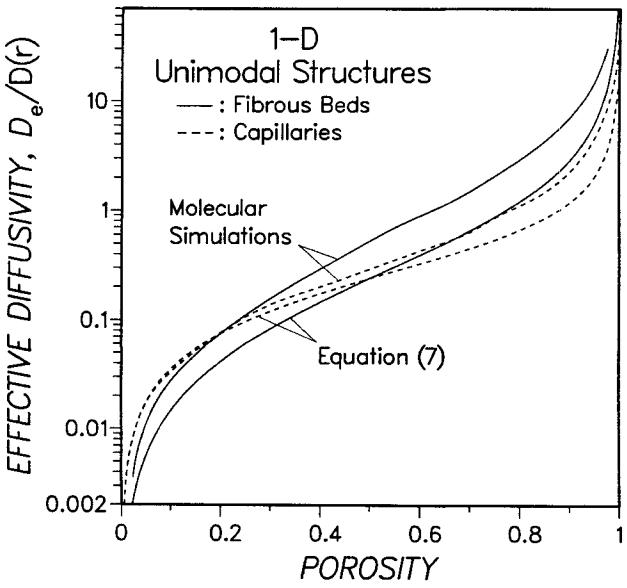

Figure 5. Orientationally average effective diffusivity of unidirectional fiber or pore structures compared with that based on average pore radius $\bar{r} = 2\epsilon/S$ for $\eta = 3$.

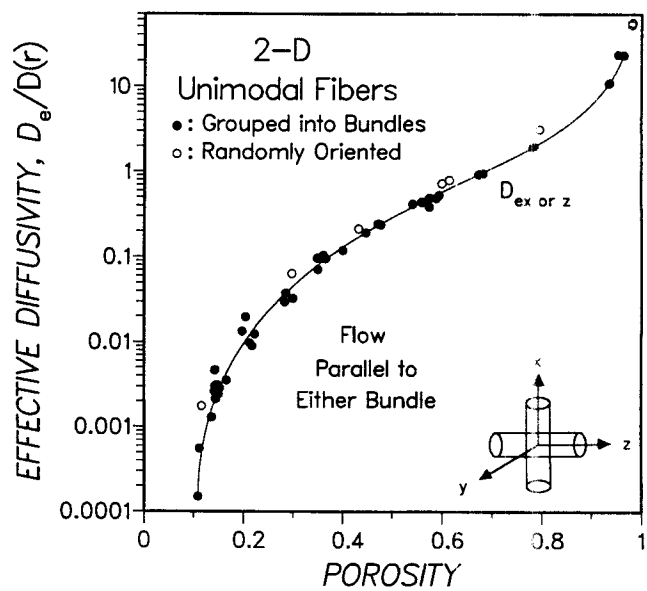

Figure 6. Effective Knudsen diffusivities parallel to plane defined by fiber directions in bidirectional fiber structures.

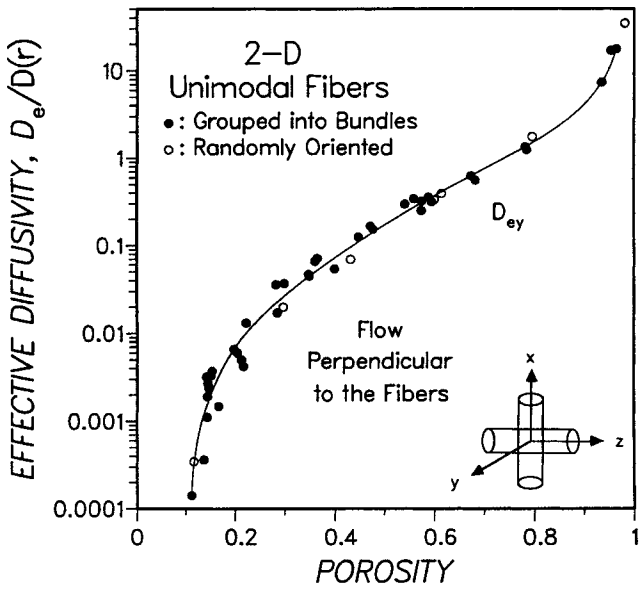

Figure 7. Effective Knudsen diffusivities perpendicular to plane defined by fiber directions in bidirectional fiber structures.

is negligible at low porosities, and hence the structure of the solid becomes equivalent to a bundle of nonoverlapping capillaries of radius $\bar{r}$ = r; see Eq. 6. Notice that the variation of $\bar{d}/r$ with the porosity is implicitly given by that of $D_e/D(r)$ predicted by Eq. 7b.

Effective diffusivities parallel to one bundle ($D_{ex \text{ or } z}$) or perpendicular to both bundles (D_{ey}) for a bidirectional fiber structure are presented in Figures 6–8. A percolation threshold is found to exist, for diffusion in all directions, at about 11% porosity, in agreement with the 89% porosity for complete fragmentation of bidirectional pore structures reported by Burganos and Sotirchos (1989b). The data points represented by open circles in Figures 6 and 7 were obtained using structures of randomly oriented fibers with their axes parallel to the (x, z) plane. The results show that the orientation of the fibers on the (x, z) plane has practically no effect on the value of the effective diffusion coefficient. The effective diffusion coefficient perpendicular to the fibers was found to be more sensitive to the realization used in the computations—compare Figures 6 and 7—and systematically smaller than that for diffusion parallel to the (x, z) plane, Figure 8. However, this difference is relatively small, indicating that a bidirectional or random in two directions fiber structure is weakly anisotropic. This result is in contrast with that obtained by Burganos and Sotirchos (1989a) for pore structures where the Knudsen diffusivity perpendicular to the pores was found to be much smaller (by more than one order of magnitude in the low-porosity range) than the Knudsen diffusivity in directions parallel to either of the pore bundles. The cause for this different behavior probably lies in the fact that straight uninterrupted paths are available for diffusion parallel to the (x, z) plane in a pore structure, while much longer, tortuous paths must be followed by molecules diffusing perpendicularly to the pores.

The variation of the effective diffusivity in the isotropic tridirectional fiber structure with the porosity is shown in Figure 9, where it is compared with the effective diffusivity based on the average radius $\bar{r} = 2\epsilon/S$, Eq. 7, for tortuosity factor η equal to 3. The dotted curve gives the diffusivity predicted by Eq. 7 when the accessible porosity and the mean intercept length of the accessible pore space, ϵ^a and $\bar{d}^a$, obtained from our simulation results, are used instead of ϵ and $\bar{d}$. Also shown in Figure 9 are the effective diffusivities computed for fiber structures constructed by positioning fibers randomly in the three-dimensional space (open circles). As in the case of bidirectional fiber structures, Figures 6 and 7, it is again seen that the orientation of the fibers—that is, whether they are randomly distributed or are grouped into three statistically identical bundles positioned in mutually perpendicular directions—has practically no effect on the value of the effective Knudsen diffusivity.

The orientationally averaged effective diffusivities for all

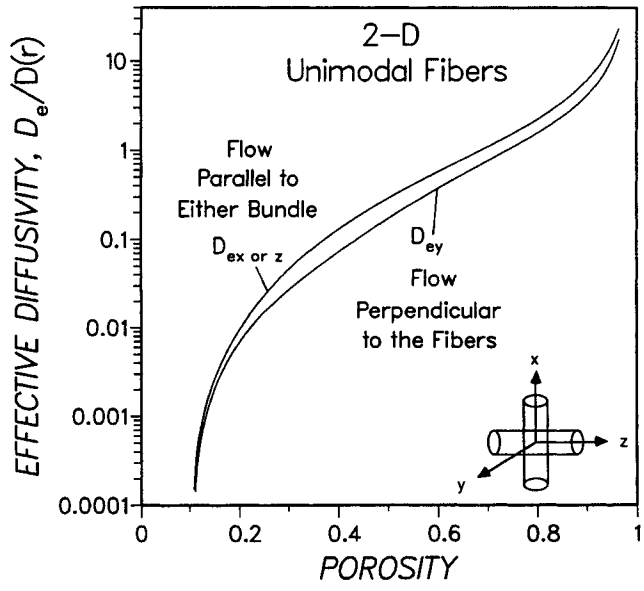

Figure 8. Comparison of results of Figures 6 and 7.

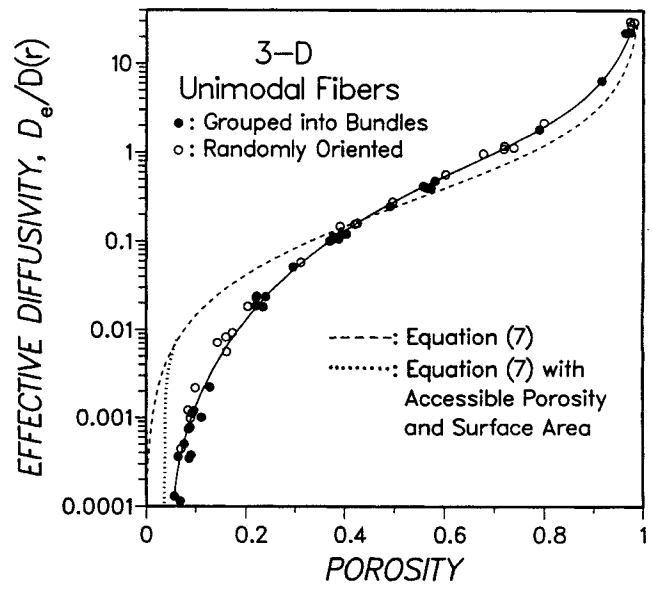

Figure 9. Effective diffusivities in tridirectional (parallel or random) fiber structures.

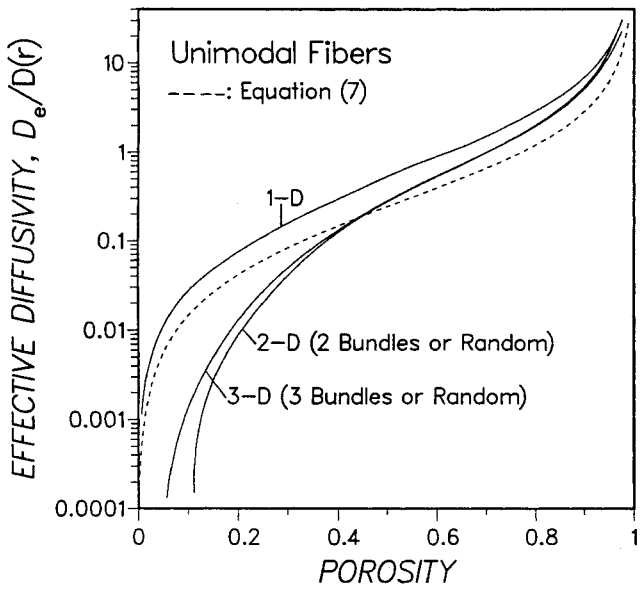

Figure 10. Comparison of orientationally averaged effective diffusivities for all directionalities.

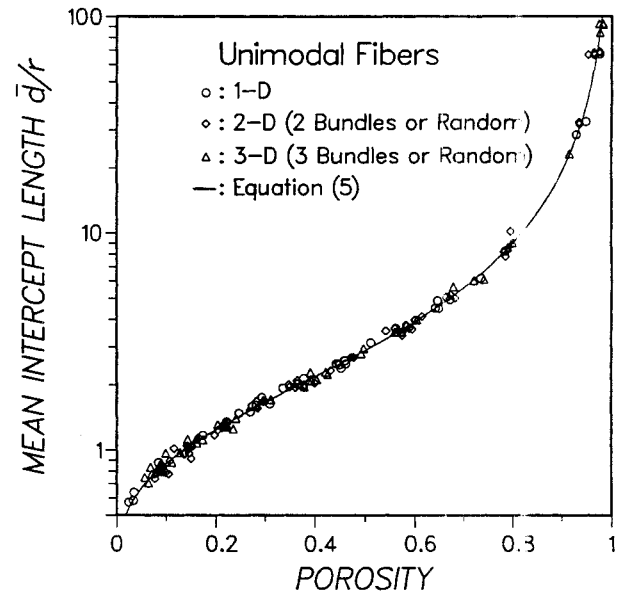

Figure 11. Computed dimensionless mean intercept length vs. porosity.

structures considered in this study are plotted as functions of porosity in Figure 10 along with the Knudsen diffusivity of Eq. 7, again for tortuosity factor η equal to 3. It is seen that in contrast to the unidirectional case, the effective diffusivities for bidirectional and tridirectional fiber structures (parallel or random) are smaller than that based on the average radius, $\bar{r}$, for porosities lower than 40–45%, indicating that their tortuosity factor relative to $D(\bar{r})$ is larger than 3 in this range. The directionality of the structure influences insignificantly the results above 50% porosity for two- and three-directional structures, but unidirectional structures give significantly higher orientationally averaged diffusivities over the whole porosity range. Bidirectional and tridirectional fiber structures present marked differences in their effective diffusivities mainly in the low-porosity region—actually, the most important for densification studies—probably because of their different percolation thresholds. The behavior seen in Figure 10 is different from that observed by Burganos and Sotirchos (1989a) for capillary structures. The orientationally averaged Knudsen diffusivity of capillary structures was found to be practically independent of the directionality and orientational distribution of the capillaries, that is, on whether they were randomly distributed or grouped into one, two, or three bundles, over the whole porosity range. It should be pointed out that in many practical applications involving anisotropic unidirectional or bidirectional fiber structures, such as chemical vapor infiltration, diffusion takes place mainly in one direction; consequently, the orientationally averaged effective diffusivities presented in this graph are of no use in such cases.

Results for structural properties

The dimensionless mean intercept length $\bar{d}/r$ and surface area Sr computed in our simulations for the realizations used to obtain the results shown in Figures 3–10 are shown in Figures 11 and 12, respectively, and compared to the theoretical results (for very large samples) given by Eq. 5 (solid curves). For the percolating bidirectional or tridirectional structures (parallel or random), the data points shown refer to the total pore space of the solid, not to its accessible part only. The mean intercept length was computed as the arithmetic mean of the paths between molecule-wall collisions, with all molecules allowed to travel for the same time. The surface area was then obtained from $\bar{d}$ and ϵ using the first part of Eq. 5: $S = 4\epsilon/\bar{d}$. The very good agreement of the simulation results for $\bar{d}$ and S with the theoretically expected values indicates that the finite sample realizations employed in our computations were statistically representative of the infinite fiber structures.

Figure 13 presents the dependence of the accessible porosity on the total porosity for the three groups of fiber structures considered in our study. (For the unidirectional fiber system,

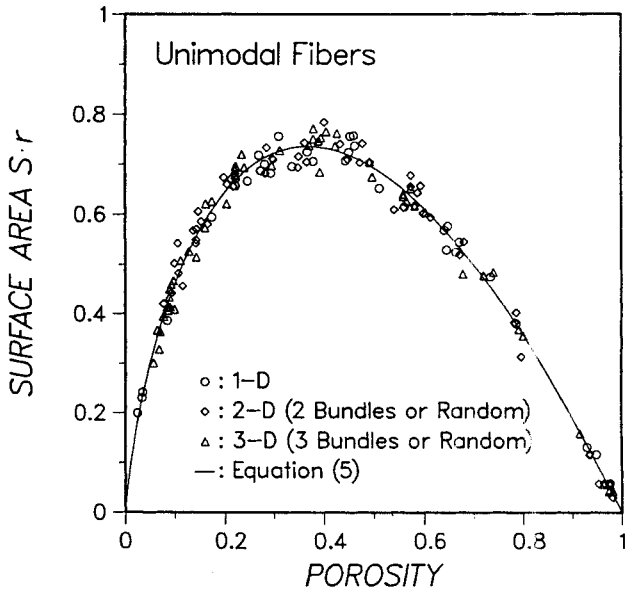

Figure 12. Computed dimensionless surface area vs. porosity.

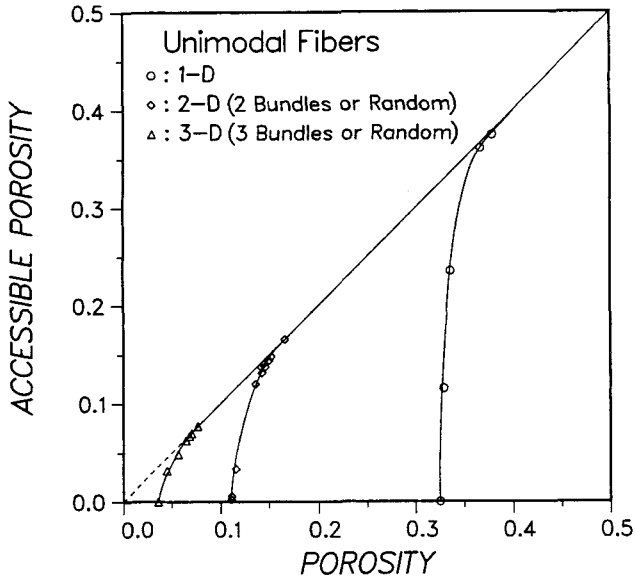

Figure 13. Variation of accessible porosity with total porosity.

accessibility is defined with respect to flow perpendicular to the fibers.) Our results were found to be in agreement with those presented by Burganos and Sotirchos (1989b) for the equivalent problem of solid-phase fragmentation in structures of cylindrical capillaries. The accessible porosity of the fiber structure was determined as the ratio of the number of molecules that are found to travel in connected areas of its pore space to the total number of molecules introduced randomly in the porous sample (Burganos and Sotirchos, 1989b). A molecule is considered to travel in the connected part of the pore space of the solid if the region of space that has been visited during its sojourn extends over one unit cell of the fiber structure, that is, if the maximal coordinate of its trajectory in the x, y, or z direction differs from the corresponding minimal coordinate by a distance greater than one unit cell side. Needless to say, the accuracy of such a computation depends strongly on the travel time or, equivalently, the travel distance of the molecules. Since the effective diffusivity of the structure decreases precipitously as the percolation threshold is approached, travel times much larger than those needed for computing effective diffusivities must be employed.

If the molecules are not given enough travel time to visit, on the average, an area larger than the unit cell, some or all of the molecules may be erroneously classified as moving in isolated parts of the pore space, leading in turn to an overestimation of the inaccessible porosity and of the percolation threshold. A rough estimate of the minimum travel time requirements, in terms of the number of molecule-wall collisions, N_c, may be obtained using the mean square displacement equation, Eq. 3a, and the equations:

$$D(r) = \frac{2}{3}\bar{v}r \tag{8a}$$

$$\bar{v}\tau = N_c\bar{d}^a \tag{8b}$$

Equation 8a is the expression for the Knudsen diffusivity, while Eq. 8b follows from the definition of $\bar{d}$ as the mean distance between molecule-wall collisions. Combining Eqs. 3a, 8a, and 8b, we obtain the equation:

$$\frac{<\xi^2>}{a^2} = \frac{4}{\epsilon^a}\left[\frac{D_e}{D(r)}\right]\left(\frac{\bar{d}^a}{r}\right)N_c\left(\frac{r}{a}\right)^2 \tag{9}$$

where a is the unit cell side. For given r/a and porosity, Eq. 9 may be used to find the number of molecule-wall collisions required to obtain a certain value of mean square displacement. For $\epsilon = 0.2$ and $r/a = 0.02$, for instance, Eq. 9 gives that in order that the molecules be displaced, on the average, from their initial positions by one unit cell side (i.e., $<\xi^2> = a^2$), about 10,000 collisions are needed in a tridirectional (parallel or random) fiber structure. (Figures 9 and 11 were used to find the values of $D_e/D(r)$ and $\bar{d}^a/r$.) The number of collisions required for such a displacement increases exponentially as the percolation threshold is approached and $D_e/D(r)$ approaches zero.

Over 200,000 collisions per molecule were used in our simulations in the vicinity of the percolation threshold to obtain the results shown in Figure 13. Considerably higher percolation thresholds, for the randomly oriented fiber structure, were recently reported by Melkote and Jensen (1989): 10–15% vs. 4% computed in our study. Their results also show formation of significant inaccessible pore space at porosities as high as 40%, while as Figure 13 shows, the fraction of inaccessible pore space is zero for porosities above 10%. The existing discrepancies between our inaccessible pore space results and those of the above study are most probably due to the relatively low number of molecule-wall collisions, only 5,000, used in the latter. Melkote and Jensen report a very strong dependence of their inaccessible porosity results on the number density of fibers (or equivalently, on the fiber radius), which lends further support to the above explanation. Specifically, they report increasing inaccessible porosity with increasing number density of fibers, that is, with decreasing fiber radius. However, the average displacement of the molecules decreases proportionally to the fiber radius for the same number of molecule-wall collisions; see Eq. 9. Therefore, more molecules may be wrongly determined as traveling in inaccessible regions as r/a is decreased if an insufficient number of collisions is used in the simulation. It should be pointed out that the effective diffusivities computed by Melkote and Jensen (1989) using transmission probabilities, to be discussed later, suggest a percolation threshold closer to our result.

Burganos and Sotirchos (1989b) used probabilistic arguments to derive a correlation that could be used to relate the fragmented solid fraction of two- or three-directional pore structures to the total porosity using the simulation results for the fragmented fraction, perpendicular to the pores, of unidirectional pores. An analogous expression can also be derived for fiber structures. If $\epsilon_d^a(\epsilon)$ ($d = 1, 2, 3$) is the inaccessible porosity of a d-directional fiber structure for porosity ϵ, this expression has the form

$$\epsilon_d^a(\epsilon) \simeq [\epsilon_1^a(\epsilon^{1/d})]^d,\ d = 2, 3 \tag{10}$$

For the percolation thresholds, Eq. 10 states that the percolation threshold of a d-directional fiber structure can be approximated by the dth power of the percolation threshold of

unidirectional fiber structures, for flow perpendicularly to the fibers. As an inspection of Figure 13 reveals, the results obtained in this study are in good agreement with the predictions of Eq. 10.

The solid and the void phases of unidirectional fiber structures percolate, perpendicularly to the fibers, at the same porosity level; consequently, their percolation threshold can be located as the largest porosity at which infinite clusters of fibers appear. A cluster identification scheme was used to identify clusters of fibers in the unit cell of unidirectional fiber structures. If any of these clusters was found to transverse the unit cell, that is, to contain boundary fibers from two opposite faces of the unit cell, the void space of the fiber structure was assumed to consist of disjoint finite regions: that is, the fibrous structure was considered impervious to diffusion. For a given realization (positions of the fiber axes in space), the porosity of the structure was varied by varying the radius of the fibers. In this way the maximum radius and minimum porosity that gave only finite clusters was located. Fiber densities ranging from 50 to 1,000 per unit cell were used in our cluster identification studies. The percolation threshold was then computed as the average of the percolation thresholds of 50 different realizations of the same number of fibers. The average percolation threshold was found to be about 0.33 and practically independent of fiber densities in the above range, in agreement with the results of past investigations (Pike and Seager, 1974). However, increasing the number of fibers in the cell tended to decrease the range in which the percolation threshold varies. The average percolation threshold and standard deviation were found to be:

No. Fibers	Avg. Perc. Thresh.	Std. Dev.
50	0.321	0.085
200	0.329	0.045
1,000	0.327	0.032

In order to reduce the scatter of our accessible porosity results and obtain an average curve for its variation with the total porosity, accessible porosities were computed working with fiber structures that would percolate exactly at the average value obtained by the cluster identification procedure. A similar approach was also followed for bidirectional and tridirectional parallel-fiber structures. Specifically, the realization of each bundle of fibers was chosen so that it would by itself percolate at the average threshold of a unidirectional fiber structure. Such an approach cannot be followed for the randomly oriented bidirectional and tridirectional structures, but the accessible porosity results for these structures proved to be considerably less sensitive to the realization.

It should be pointed out that even if the structure of a porous medium can be represented by randomly overlapping fibers, the data of Figure 13 are not representative of the variation of the inaccessible porosity of the fibrous structure with the porosity during densification (by chemical vapor infiltration, for instance). Regions of inaccessible pore space should not participate in the chemical reaction once they are formed. However, since the structures used to compute the results of Figure 13 are constructed at all porosities using overlapping cylindrical fibers, it is essentially assumed that solid deposition occurs at all points of the internal surface area at all porosities. The "actual" accessible porosity vs. total porosity (ϵ^a vs. ϵ) curves are therefore expected to be shifted to the right relative to the curves shown in Figure 13, with the "actual" percolation threshold of each case appearing between the point where noticeable formation of inaccessible porosity starts to take place and the threshold of Figure 13. However, since formation of inaccessible pore space in the uncorrelated percolation problem, Figure 13, is completed within a narrow range of porosity, the differences of the "actual" ϵ^a vs. ϵ curves from those of Figure 13 will most probably be small. The investigation of the correlated percolation problem is among the subjects of our current research efforts.

Comparison with estimates of upper bounds

Using variational principles, upper bounds can be derived for the Knudsen effective diffusivity of a porous medium (Strieder and Aris, 1973). The bound is written in terms of certain averages depending on the geometry of the void-solid interface. For certain classes of porous media these averages can further be expressed in terms of the average properties of the structure (e.g., porosity and internal surface area). The upper bound on the effective diffusivities of porous media is usually given in terms of the permeability coefficient C, defined by the equation

$$\Pi \equiv \frac{JL}{|\Delta p|} \equiv C \frac{\bar{d}\epsilon}{\sqrt{2\pi MRT}} \tag{11}$$

J is the diffusion flux, and L is the distance across which a pressure difference $|\Delta p|$ or concentration difference $|\Delta c|$ is maintained.

Using the definitions of D_e, $\bar{d}$, and $\bar{v}$,

$$D_e \equiv \frac{JL}{|\Delta c|} = \Pi RT \tag{12a}$$

$$\bar{d} = \frac{4\epsilon}{S} \tag{12b}$$

$$\bar{v} = \sqrt{\frac{8RT}{\pi M}} \tag{12c}$$

one can readily transform Eq. 11 into an expression relating the effective diffusivity D_e to the permeability coefficient C:

$$D_e = C \frac{\epsilon^2}{S} \bar{v} \tag{13}$$

Comparing Eqs. 7 and 13, we see that the variable tortuosity that must be used in Eq. 7 to make its predictions agree with our simulation results is $\eta = 4/(3C)$. The values of C that correspond to our simulation results can be obtained from the dimensionless diffusivities and structural properties of Figures 3-12 using the equation (cf. Eq. 13)

$$C = \frac{2}{3}\left(\frac{Sr}{\epsilon^2}\right)\left[\frac{De}{D(r)}\right] \tag{14}$$

Faley and Strieder (1987) considered the problem of Knudsen

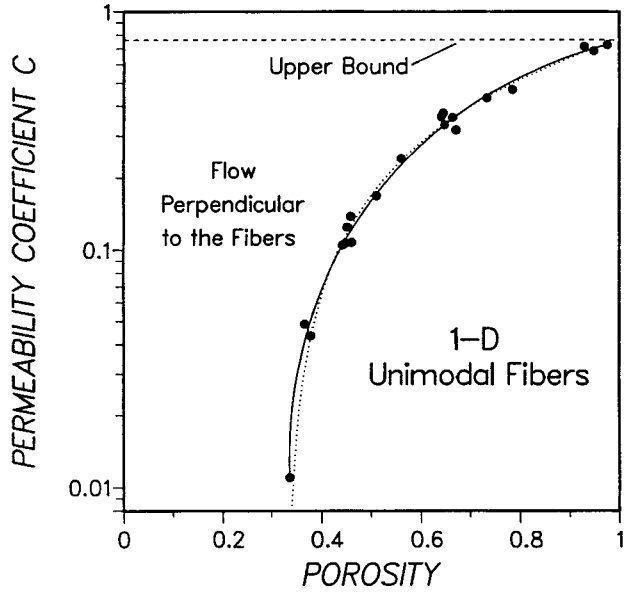

Figure 14. Variation of permeability coefficient with porosity in unidirectional fibers.

Dotted curve obtained from Eq. 15 using parameters of Table 1

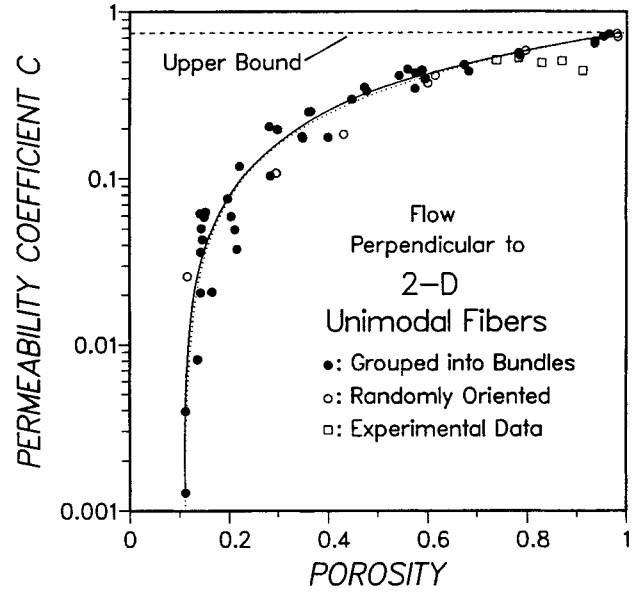

Figure 15. Variation of permeability coefficient with porosity in bidirectional (parallel or random) fibers.

Dotted curve obtained from Eq. 15 using parameters of Table 1

diffusion in a direction perpendicular to the fibers of a unidirectional fiber structure. They derived the bound $C \leq 0.763$, which is compared in Figure 14 (dashed line) with the C vs. ϵ results of Figure 3 using Eq. 14. It is seen that our simulation results approach the Faley and Strieder bound at the limit of a very dilute bed ($\epsilon \rightarrow 1$), but significant deviations are observed at low or moderate porosity values. In a later paper, Faley and Strieder (1988) derived upper bounds for the Knudsen permeability for two or more configurations of flow through fibrous beds. When the fiber axes are oriented at random, perpendicular to the direction of flow, Figure 7, the upper bound on C is found to be 0.7489, while for beds of fibers oriented randomly in three directions, the well-known result of Derjaguin ($C \leq 12/13$) is obtained. Figures 15 and 16 compare our simulation results for fibers distributed randomly in two and three directions, respectively, with the above permeability bounds. It is again seen that our computational results are in excellent agreement with the upper bounds for very dilute beds ($\epsilon \rightarrow 1$). However, the numerically computed Knudsen permeabilities decrease monotonically with decreasing porosity, becoming identically zero at the percolation thresholds.

In order to render our simulation results readily usable by people working in areas involving diffusion in fibrous beds, such as the fabrication of ceramic composites by chemical vapor infiltration, we searched for simple, one-parameter correlations that would provide satisfactory approximations to the computed effective diffusivities using the known structural properties of the fibrous structures. Various one-parameter correlations were tested, and the one that appeared to work the best for all cases examined in this study was of the form

$$C = C_{max} \left(\frac{\epsilon - \epsilon_p}{1 - \epsilon_p} \right)^{\alpha} \tag{15}$$

in terms of the permeability coefficient C, Eq. 13, or equivalently, of the form

$$\eta = \eta_{min} \left(\frac{1 - \epsilon_p}{\epsilon - \epsilon_p} \right)^{\alpha} \tag{16}$$

in terms of the tortuosity, Eq. 7b, with ϵ_p being the percolation threshold of the fiber structure in the direction of diffusion. The dotted curves of Figures 14, 15, and 16 give the permeability coefficient vs. porosity curves predicted by Eq. 15 for the case considered in each figure, using the values of α listed

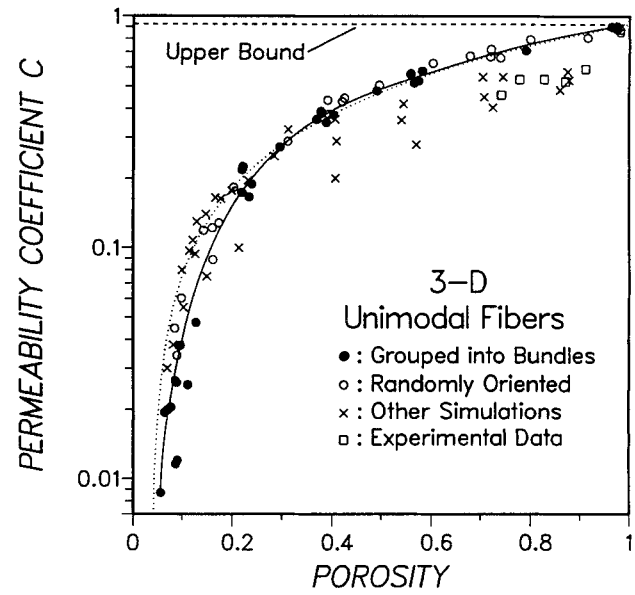

Figure 16. Variation of permeability coefficient with porosity in tridirectional (parallel or random) fibers.

Dotted curve obtained from Eq. 15 using parameters of Table 1

Table 1. Parameters Used in Eqs. 15 and 16

	Direction	C_{max}	η_{min}	ϵ_p	α
1-D	z	2.43	0.549	0	0
	x, y	0.763	1.747	0.33	1.099
2-D	y	0.749	1.780	0.11	1.005
	x, z	1.16	1.149	0.11	0.954
3-D	x, y, z	12/13	13/9	0.037	0.921

in Table 1. Also listed in the table are the maximum values of the permeability coefficient and minimum values of tortuosity for each case.

The value of α was determined using a parameter estimation procedure based on the minimization of the square error between the permeability coefficients computed from our simulation results using Eq. 14 and those predicted by Eq. 15. The C_{max} (or η_{min}) values of Table 1 for unidirectional and bidirectional (1-D and 2-D) structures perpendicular to the fibers and tridirectional fibers in any direction are those obtained through variational principles. The listed values for 1-D and 2-D structures parallel to one bundle of fibers were obtained from our simulation results. All η vs. porosity results obtained in this study are summarized in Figure 17. Interestingly enough, the tortuosity factor parallel to the fibers of unidirectional structures appears to be invariant over the whole porosity range, which is exactly what the parameters of Table 1 also suggest. To emphasize this result, the obtained (η, ϵ) pairs for diffusion parallel to the fibers of 1-D structures are also shown in the figure. The solid curves shown in this figure, as well as in all previous figures, were obtained through cubic spline approximation to the simulation data using software provided with the graphics package used to plot our results.

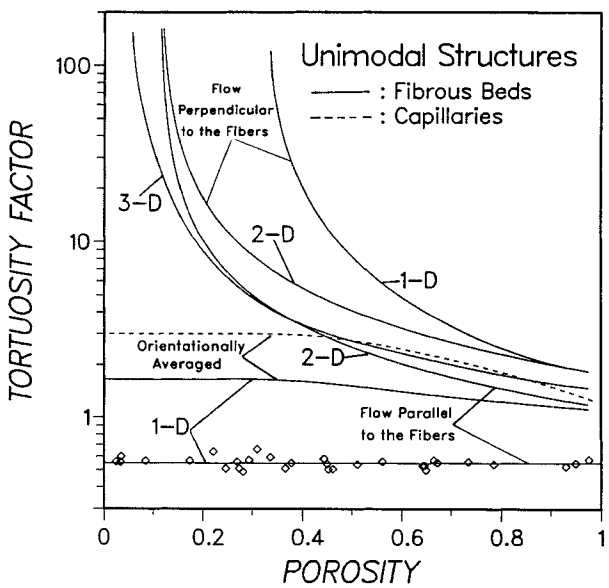

Figure 17. Variation of tortuosity factor, based on diffusivity for $\bar{r} = 2\epsilon/S$, with porosity for all cases.

Comparison with experimental data and simulation results of other studies

The experimental data shown in Figures 15 and 16 are based on permeability measurements performed by Brown (1950). The data of Figure 15 were obtained for flow in a bed of disks stamped out of thin sheets of glass wool fibers and laid on top of each other in the sample holder in such a manner that the fibers were almost perpendicular to the tube axis, that is, to the direction of gas flow. For the second series of measurements, presented in Figure 16, the fibers were cut into 1 cm lengths and placed in the fiber holder with no preferred orientation. Brown performed his experiments in the slip flow regime. By plotting the measured flow rates vs. the mean pressure in the bed, he determined the viscous and slip contributions to the total flow rate from the slope and intercept of the resulting straight line. Carman (1956) used Brown's results to determine the value of the tortuosity factor η in Eq. 7 (k'/δ in Carman's symbols) on which we based the permeability factor C plotted in Figures 15 and 16 ($C = 4/[3\eta]$).

The experimentally measured permeability factors are smaller than those computed numerically, but the differences are smaller for the bidirectional random-fiber structures. It is interesting to note that Brown himself expressed doubts as to whether the fibers were truly randomly oriented in his second series of measurements (Brown, 1950). However, even if the experimental data are correct, it is debatable whether the same tortuosity factor can be used for pure Knudsen diffusion and the slip contribution during slip flow. Experiments with small, nearly spherical synthetic crystals (Barrer and Grove, 1950) gave tortuosity factors 18% higher in the slip region than in the Knudsen regime, while Carman's (1956) experiments in powder beds suggested lower tortuosity factors for slip flow.

Figure 15 also presents simulation results for Knudsen diffusion in structures of randomly oriented fibers, obtained by Melkote and Jensen (1989) using the transmission probability method (Davis, 1960; Abbasi, 1981; Burganos and Sotirchos, 1988). There is good agreement between their results and those obtained in this study at low porosities, but significant differences are observed in the high-porosity region. These differences cannot be attributed to the different methods used in the two studies because using the transmission probability method, we obtained results identical to those of the mean square displacement method for the fiber structures used in our study. (We chose the mean square displacement method for the bulk of our computations because it requires, in general, less computer time and, in contrast to the transmission probability method, is capable of giving both the orientationally averaged effective diffusivity and the diffusivities in other directions with a single set of simulation computations.)

The different results of Melkote and Jensen (1989) could be due to the use of periodic boundary conditions for the molecular trajectories on a nonperiodic unit cell. Specifically, they reintroduced into the unit cell molecules reaching one of its lateral faces through the opposite face, retaining their direction of travel. Since the unit cell is nonperiodic, its parallel faces are practically unrelated to each other. Consequently, molecules reintroduced in the unit cell as above have probability ϵ of entering the void of the unit cell and $(1 - \epsilon)$ of entering the solid phase. According to Melkote and Jensen, "The molecule is then sent to the closest cylinder such that its intersection with the trajectory is within the cell boundaries." In other

words, the $(1 - \epsilon)$ fraction of molecules that fall in the solid phase are allowed to "travel" within the solid fibers until they reach a point of the void-solid interface lying in the unit cell (R. R. Melkote, personal communication, 1990). This treatment of the diffusing molecules modifies drastically the transport and accessibility characteristics of the fiber structure since by "traveling" through the solid phase, molecules originating from a certain point can now visit areas that would otherwise be inaccessible to them.

Summary and Conclusions

A numerical investigation of the problem of Knudsen diffusion in structures of randomly overlapping fibers of various orientation distributions was carried out. The axes of the fibers were randomly distributed in $d(d = 2$ or $3)$ directions or grouped into $d(d = 1, 2,$ or $3)$ mutually perpendicular bundles of parallel, randomly overlapping fibers (d-directional, random or parallel fiber structures). Effective diffusivities were computed using the mean square displacement of molecules traveling in the porous medium for large travel times. It was determined using a Monte Carlo simulation process based on following the trajectories of a large number of molecules, each traveling independently, introduced randomly in a finite sample of the fiber structure. Using a method proposed by Burganos and Sotirchos (1989b), the computed molecular trajectories were also used to determine the accessible porosity and internal surface area of the structures. Appropriate boundary conditions were imposed on the faces of the finite sample in order to be able to obtain simulation results representative of the infinite medium. In order to check the results of the mean square displacement method, effective Knudsen diffusivities were also computed by numerical integration of an analytical expression for straight tubes (Kennard, 1938), applicable to diffusion parallel to the fibers of unidirectional structures, and by using Monte Carlo estimates of the transmission probability of molecules through a pair of parallel planes.

Our results showed strong dependence of the effective Knudsen diffusivity on the directionality of the fiber structures at low and intermediate porosity values, including the orientationally averaged diffusivities for the anisotropic one- and two-directional structures. This result is in sharp contrast with the conclusions of Burganos and Sotirchos (1989a) for capillary structures, where the directionality had practically no effect on the orientationally averaged effective diffusivity. However, the effective diffusivities were found to be independent of the orientation of the fibers in two or three directions, that is, on whether they were randomly distributed or grouped into two or three bundles of parallel fibers. With respect to the diffusion coefficient based on the average radius $\bar{r} = 2\epsilon/S$, the orientationally averaged tortuosity factor of unidirectional fiber beds is smaller than 3 at all porosities, while for fibers distributed randomly in two or three directions this happens for porosities above 40–45%. As the porosity approaches unity, the tortuosity factor approaches the corresponding lower bound for each case derived using variational principles (Faley and Strieder, 1987, 1988).

The percolation threshold of tridirectional (parallel or random) fiber beds—that is, porosity at which the void space forms only finite regions and mass transport cannot take place—is lower than that of bidirectional or random in two directions beds (0.04 vs. 0.11). As a result, the latter, which are weakly anisotropic, have lower effective diffusivities. This suggests that it may be advantageous to use three-dimensional random or woven structures instead of cloth layups as preforms in chemical vapor infiltration. Unidirectional structures present a much higher percolation threshold for transport perpendicular to the fibers (~ 0.33), but since they are always accessible parallel to the fibers, their orientationally averaged effective diffusivity is much higher than those for other directionalities.

Notation

Symbols that do not appear here are defined in the text.

a = side of cubic unit cell, m
C = permeability coefficient, Eq. 11
d = directionality of fibers ($d = 1, 2,$ or 3)
$\bar{d}$ = mean intercept length ($\bar{d} = 4\epsilon/S$), m
$D(r)$ = Knudsen diffusivity in a cylindrical capillary of radius r, m^2/s
D_e = effective diffusivity, m^2/s
l_i = length of axes per unit volume of fiber of radius r_i, m/m^3
M = molecular weight, kg/kmol
N_c = number of molecule-wall collisions
r = fiber radius, m
$\bar{r}$ = average pore radius ($\bar{r} = 2\epsilon/S$), m
R = ideal gas constant, J/kmol·K
S = internal surface area, m^2/m^3
T = temperature, K
$\bar{v}$ = mean thermal speed of molecules, m/s

Greek letters

α = parameter, Eqs. 15, 16
ϵ = porosity
ϵ_d^a = accessible porosity of a d-directional fiber structure
η = tortuosity factor
$<\xi^2>$ = mean square displacement, m^2
τ = travel time

Superscripts

a = accessible structural properties

Subscripts

x, y, z = x, y, or z direction

Literature Cited

Abbasi, M. H., "A Monte Carlo Simulation of the Diffusion of Gases and Radiant Heat Transfer in Porous Solids," PhD Thesis, Univ. California, Berkeley (1981).

Barrer, R. M., and D. M. Grove, "Flow of Gases and Vapours in a Porous Medium and Its Bearing on Adsorption Problems," *Trans. Faraday Soc.*, **47**, 826 (1950).

Brown, J. C., "Determination of the Exposed Specific Surface of Pulp Fibers from Air Permeability Measurements," *TAPPI*, **33**, 130 (1950).

Burganos, V. N., and S. V. Sotirchos, "Simulation of Knudsen Diffusion in Random Networks of Parallel Pores," *Chem. Eng. Sci.*, **43**, 1685 (1988).

Burganos, V. N., and S. V. Sotirchos, "Knudsen Diffusion in Parallel, Multidimensional or Randomly Oriented Capillary Structures," *Chem. Eng. Sci.*, **44**, 2451 (1989a).

Burganos, V. N., and S. V. Sotirchos, "Fragmentation of Random Pore Structures," *Chem. Eng. Commun.*, **85**, 95 (1989b).

Carman, P. C., *Flow of Gases through Porous Media*, Butterworths, London (1956).

Davis, D. H., "Monte Carlo Simulation of Molecular Flow Rates

through a Cylindrical Elbow and Pipes of Other Shapes," *J. Appl. Phys.*, **31**, 1169 (1960).
Faley, T. L., and W. Strieder, "Knudsen Flow through a Random Bed of Unidirectional Fibers," *J. Appl. Phys.*, **62**, 4394 (1987).
Faley, T. L., and W. Strieder, "The Effect of Random Fiber Orientation on Knudsen Permeability," *J. Chem. Phys.*, **89**, 6936 (1988).
Kennard, E. H., *Kinetic Theory of Gases*, McGraw-Hill, New York (1938).
Melkote, R. R., and K. F. Jensen, "Gas Diffusion in Random Fiber Structures," *AIChE J.*, **35**, 1942 (1989).
Pike, G. E., and C. H. Seager, "Percolation and Conductivity: A Computer Study. I," *Phys. Rev. B.*, **10**, 1421 (1974).
Rahman, A., "Correlations in the Motion of Atoms in Liquid Argon," *Phys. Rev.*, **136**, A405 (1964).
Stinton, D. P., T. M. Besmann, and R. A. Lowden, "Advanced Ceramics by Chemical Vapor Deposition Techniques," *Ceramic Bull.*, **67**, 350 (1988).
Strieder, W. and R. Aris, *Variational Methods Applied to Problems of Diffusion and Reaction*, Springer, New York (1973).
Sotirchos, S. V., and M. M. Tomadakis, "Modeling Transport, Reaction, and Structure Evolution during Densification of Cellular or Fibrous Preforms," *Chemical Vapor Deposition of Refractory Materials*, 73, T. M. Besman and B. M. Gallois, ed., Mat. Res. Soc., Pittsburgh (1990).

Manuscript received Mar. 22, 1990, and revision received Oct 30, 1990.